JOURNAL OF GEOPHYSICAL RESEARCH, VOL. 104, NO. A5, PAGES 10,335–10,344, MAY 1, 1999

Predictability of *Dst* index based upon solar wind conditions monitored inside 1 AU

G. M. Lindsay[1] and C. T. Russell

Institute of Geophysics and Planetary Physics, University of California, Los Angeles

J. G. Luhmann

Space Sciences Laboratory, University of California, Berkeley

Abstract. The formula of *Burton et al.* [1975] provides a quick and simple means by which the strength of the ring current and the *Dst* index can be calculated based solely on upstream solar wind density, velocity, and the north/south component of the magnetic field. Solar wind data from ISEE 3, the Pioneer Venus Orbiter, and Helios A are used to show how well *Dst* predictions based on the Burton et al. formula match *Dst* observations for upstream monitors at various heliospheric distances. It is shown that a solar wind monitor that provides a substantial geomagnetic forecast lead time, with usable predictions of the characteristics of the solar wind, can be stationed ~0.7 AU if it is near the ecliptic plane and within 10° east to 5° west of the Earth-Sun line. It is also shown that the Burton et al. formula predicts equally well the *Dst* index resulting from the passage of disturbed solar wind, associated with either interplanetary coronal mass ejections or stream-interaction regions. A solar sail-type spacecraft is proposed as the ideal monitor for forecasting purposes.

1. Introduction

For the purposes of forecasting geomagnetic storms, it is desirable to make predictions with the longest lead time possible. Linear prediction filtering and recurrence/persistence techniques have been used for a forecast lead time of ~27 days [*Bartels*, 1932; *Clauer et al.*, 1981; *Bargatze et al.*, 1985]. These techniques are useful during the declining phase of solar activity when the stream structure of the solar wind is only slowly evolving. Recurrence forecast methods do not account for newly developing streams or transient solar activity that may effect the Earth's geomagnetic environment. In practice, it is not possible to predict activity associated with interplanetary coronal mass ejections (ICMEs) that are responsible for the largest terrestrial disturbances [*Lindsay et al.*, 1995]. To predict the potential effects of the most recent solar activity (e.g., ICMEs), space weather forecasters presently observe the optical and magnetic characteristics of the solar surface in an attempt to forecast the state of the geomagnetic environment approximately 4 days later (where ~4 days is the average transit time of the solar wind between the Sun and 1 AU). The true forecast lead time will be a function of the velocity of the solar wind, and the potential strength of the geomagnetic storm will depend upon the solar wind velocity and density as well as the strength of the southward component of the interplanetary magnetic field (IMF) [*Akasofu*, 1964; *Siscoe*, 1966; *Hirshberg and Colburn*, 1968; *Russell et al.*, 1974]. Predictions of solar wind conditions at 1.0 AU based on solar observations [*Hoeksema*, 1992; *Marubashi*, 1986] are affected by changes in solar wind conditions between the Sun and Earth. The best way to forecast interplanetary conditions at Earth is to have a solar wind monitor on the streamline that intersects Earth. The closer the monitor is to Earth and to the Earth-Sun line, the more accurate the prediction of geomagnetic activity will be. The closer the monitor is to the Sun, the greater the lead time of the prediction will be. It is the purpose of this paper to provide an assessment of the effect of changing distance on the quality of geomagnetic activity forecasts using presently available data.

Burton et al. [1975] provided a relatively simple formula that allowed the accurate prediction of ring current strength and the *Dst* index based on upstream solar wind conditions near 1 AU. The assumed sources of change in the strength of the ring current are, first, the amount of injection ($F(E)=d(Ey-0.5)$, where $d = -1.5\text{x}10^{-3}$ nT((mV m^{-1})s)$^{-1}$ and Ey is the y GSM component of the interplanetary electric field), and, second, the amount of decay which is proportional to the strength of the ring current. In their formula, $dDst_0/dt = F(E)-aDst_0$, where $F(E)$ is nonzero only for southward solar wind magnetic fields (the half-wave rectifier assumption) and "a" is an empirically derived constant representing the fractional loss of ring current per unit time ($3.6\text{x}10^{-5}$ s^{-1}). When the IMF is southward and the solar wind convective electric field (VB_z) is sufficiently strong such that $F(E)$ exceeds $aDst_0$, the ring current is energized. When the IMF turns northward, $F(E)$ is zero and the ring current is no longer energized, decaying and becoming weaker. *Dst* is the perturbation of the horizontal component of the Earth's magnetic field as measured by midlatitude ground stations in nanoteslas. It is the sum of the ring current and the magnetopause currents and

[1]Now at HQ AFSPC/DRFS, Peterson Air Force Base, Colorado.

Paper number 1999JA900010.
0148-0227/99/1999JA900010$09.00

equals zero when the magnetopause currents and ring currents have their quiet-day values. *Burton et al.* [1975] obtained their ring current value by subtracting from *Dst* the correction term $b(\rho V^2)^{1/2}$-c. The constants "b" and "c," also empirically derived, represent the response to dynamic pressure changes in the solar wind (15.8 nT(nPa)$^{-1/2}$) and the quiet-day currents (20 nT), respectively. Large, negative *Dst* characteristic of geomagnetic storms occurs when the ring current is strong (i.e., during periods of large, duskward *Ey*). Positive *Dst* occurs when the magnetopause currents are strong and the ring current is weak (i.e., during periods of strong solar wind dynamic pressure and northward B_z).

Forecasting *Dst*, then, is essentially a matter of predicting the solar wind conditions at the front of the magnetosphere. *Burton et al.* [1975] tested their *Dst* prediction formula during geomagnetically active periods using Explorer 34 solar wind and IMF data observed at the nose of the magnetopause (~1.0 AU). However, it has not been tested over an extended period of time, nor has the observation site for the IMF been evaluated at any point other than just outside the magnetopause. Particularly, the ISEE 3 data at 0.98 AU have not been used in such a test. The capability of using data well inside 1 AU provides even greater lead time. If the *Burton et al.* [1975] formula could be used on solar wind data observed near 0.3 AU, the forecast lead time would increase to about 3 days for average solar wind and ~1.5 days for an 800-km s^{-1} solar wind.

Unlike any previous study, this study examines the range of applicability of the Burton et al. formula by applying it to solar wind observations from ISEE 3, Pioneer Venus Orbiter (PVO), and Helios A to evaluate the usefulness of the Burton et al. formula during both geomagnetic storm and geomagnetically quiet times and to determine the usefulness of the Burton et al. formula using solar wind observed inside 1 AU. It is found that the simple formula devised by *Burton et al.* [1975] is remarkably robust and predicts the *Dst* index well during both geomagnetic storm and quiet periods using measurements near the L1 libration point despite the occasional differences seen in the direction of the IMF between this site and Earth [e.g., *Russell et al.*, 1980; *Crooker et al.*, 1982]. Moreover, geomagnetically useful predictions with 24-hour forecast lead times can be achieved with an upstream solar wind monitor as far inside 1.0 AU as 0.7 AU during both geomagnetic storm and geomagnetically quiet times, but the prediction is less accurate during all conditions for more distant monitors closer to the Sun. The apparent reason for this modicum of predictability despite the large distances involved is that it is the long scale sizes in the IMF that control the ring current energization. Finally, the Burton et al. formula is found to work well regardless of the source of the conditions in the solar wind (e.g., stream interactions or coronal mass ejections).

2. Examples

2.1 ISEE 3: 1.0 AU Monitor

Plates 1 and 2 show comparisons between *Dst* predicted from the *Burton et al.* [1975] formula (red trace) using ISEE 3 solar wind data near 1.0 AU and that observed (black trace) by midlatitude ground stations. The observed *Dst* (obtained from the National Space Science Data Center database) has a 1-hour resolution, while the *Dst* predicted by ISEE 3 has a 5-min resolution. ISEE 3 provides about a 45-min lead time between *Dst* prediction and *Dst* observation at 1.0 AU. The predicted *Dst* shown in Plates 1 and 2 has not been delayed by the expected solar wind convection time between ISEE 3 and 1.0 AU. We have not attempted to predict this delay because the convection time depends on the location of ISEE 3 perpendicular to the streamline of the solar wind passing through the stagnation point and the orientation of the structure convected past ISEE 3. This orientation will be different for coronal mass ejections (CMEs) and stream interaction regions.

Plate 1 shows a 540-day comparison obtained from the ISEE 3 interplanetary data set for the mission period when the plasma analyzer was functioning (September 1, 1978, to February 23, 1980). To highlight any recurrent features, the length of each data strip is 27 days (approximately one solar rotation). At this resolution, *Dst* predicted by the Burton et al. formula is in excellent agreement with the actual *Dst* observations. For most of the time, the predicted and observed *Dst* values differ only slightly (an average amount of only ~5 nT). However, there are isolated periods where the agreement in magnitude differs by an average of ~50 nT (September 29-30, 1978, February 21-24, 1979, April 24-28, 1979 and July 3-9, 1979, hereafter referred to as cases a, b, c, and d, respectively). In cases a and d, the observed *Dst* is less disturbed than predicted indicating that the ring current was less energized than predicted. This difference suggests that less reconnection occurred than assumed by the form of $F(E)$ in the Burton et al. formula. In cases b and c, the observed *Dst* is more disturbed than predicted, indicating that more ring current energization occurred than predicted.

These occasional differences suggest that additional factors are affecting the $F(E)$ in the Burton et al. formula. Two possible factors are the beta of the magnetosheath plasma and the dynamic pressure of the solar wind. High-beta values in the magnetosheath have been found to reduce the rate of reconnection [*Paschmann et al.*, 1986; *Scurry and Russell*, 1991; *Scurry et al.*, 1994]. The beta in the magnetosheath is controlled principally by the solar wind magnetosonic Mach number and partially by solar wind beta. During each of these four periods, the solar wind was characterized by extremely low solar wind beta (beta<0.4). Beta in this low regime is most often associated with the passage of an ICME [*Klein and Burlaga*, 1982]. Indeed, during a, b, and c, CMEs passing by 1.0 AU were identified by *Gosling et al.* [1987]. The low-beta solar wind associated with case d is due to the passage of the high-speed portion of a fast/slow stream interaction region characterized by lower than average densities (~3 cm^{-3}) and higher than average magnetic fields (~12 nT). Solar wind beta does not appear to be a factor in any of our four cases.

The solar wind magnetosonic Mach number also helps determine the value of beta in the magnetosheath, and it too varies from case to case. In cases a and d, the magnetosonic Mach number was relatively low (~2-3) during a period when the observed *Dst* was less than predicted, implying reconnection was weaker than expected. For cases b and c, the magnetosonic Mach number was near average to slightly higher than average (~4-6) when the observed *Dst* was greater than predicted, implying reconnection was stronger than expected. This is opposite to the behavior expected from the study of *Scurry and Russell* [1991]. Their results indicate that the efficiency of reconnection is nearly constant for Mach numbers less than about seven and that the efficiency drops above a Mach number of seven when the beta in the magnetosheath becomes high. Again, we draw the conclusion that magnetosheath beta variations do not affect our four cases.

Dynamic pressure has been found to be an important factor in enhancing geomagnetic activity and, by inference, the rate of

reconnection [*Scurry and Russell*, 1991]. Common between cases b and c, where more ring current energization than predicted was observed, is high solar wind dynamic pressure (~10-30 nPa) associated with large IMF and a high likelihood of B_z being southward. Common between cases a and d, where less ring current energization than predicted was observed, is average to low solar wind dynamic pressure (~1-3 nPa) associated with large IMF magnitudes and an equal likelihood of B_z being either northward or southward. Thus varying solar wind dynamic pressure appears to be the cause of the varying efficiency of coupling in our four cases.

Plate 2 shows a particular 27-day interval extracted from the 540-day period in Plate 1. In this enlargement, it is easier to see how well the variation and level of activity are predicted using the formula of Burton et al. with ISEE 3 upstream solar wind measurements. (As noted above, the one exception in this interval occurs on February 21-24, 1979, a period of high solar wind dynamic pressure.) During this time, the times of the increases and decreases in *Dst* are well predicted, but the predicted level of activity (magnitude) is less than that observed. Interplanetary shocks (solid arrows) and coronal mass ejections (open arrows) as identified by *Gosling et al.* [1987] using bidirectional electron signatures, are indicated. Each interplanetary shock produces a sharp increase in both predicted and observed *Dst*. The first ICME produces a large decrease in observed *Dst* that is not predicted. The second and third ICMEs produce decreases in *Dst* that are correctly predicted.

2.2 Pioneer Venus Orbiter: 0.7 AU Monitor

Plate 3 shows a 27-day comparison between predicted *Dst* using 10-min resolution solar wind data measured at 0.7 AU with Pioneer Venus Orbiter (PVO) and observed *Dst* at 1.0 AU from June 1-28, 1980. During this period, PVO is within ±10° of the Earth-Sun line and close to the intersection of the Venus orbital plane with the ecliptic plane. It is assumed that solar wind velocity does not vary appreciably between 0.7 AU and 1.0 AU and that the values of ρ and B_z vary as r^{-2} and r^{-1}, respectively. In this case, the solar wind monitor is 0.3 AU inside 1.0 AU. At a typical solar wind velocity of about 450 km s^{-1}, the solar wind plasma would take about 24 hours to reach Earth from 0.72 AU. We have not taken this delay into account in Plate 3. Thus the predicted trace shown should be ~1 day in advance of the observed *Dst* at 1.0 AU. Over the initial 10 days of this period, changes in the magnetic field have very similar magnitudes and occur nearly simultaneously. The recovery of the PVO-predicted *Dst* occurred on day 164, 2 days ahead of when it occurred at Earth. Thereafter *Dst* is predicted to be quiet, and it is. So during this one period of coalignment, measurements at 0.72 AU could be used to predict the general level of activity although not the specific timing to better than a day.

This period of good correspondence occurred even though there were several transient disturbances in the solar wind. During the period shown, two stream interactions (on June 5 and June 20, 1988) and two ICMEs (on June 10 and June 26, 1980) are observed at 0.7 AU. The first stream interaction is associated with a predicted increase in *Dst* to positive values. The second stream interaction produces only a slight increase in *Dst* to ~0 nT. After both stream interactions, *Dst* decreases and becomes negative. The first stream interaction region produces a significant decrease in *Dst*, while only a slight decrease in *Dst* occurs after passage of the second stream interaction region. This behavior is predicted as well as observed. In both cases, the maximum magnitude of positive *Dst* is underpredicted. The first stream interaction appears to have been more conducive to ring current energization (indicated by *Dst*<0) because of more southward B_z. The second stream interaction is more conducive to sustained magnetospheric compression as suggested by the substantial period of *Dst*>0 resulting from its higher dynamic pressures.

Both ICMEs are associated with predicted and observed periods of large, negative *Dst*. The ICME observed during the first period has a peak velocity of ~600 km s^{-1} and southward B_z of ~20 nT. The second ICME has a peak velocity of ~400 km s^{-1} and southward B_z of ~15 nT. The longer duration of negative *Dst* following the first ICME probably occurred because B_z was southward for a longer period during the first ICME than the second ICME.

2.3 Helios A: 0.6 to 1 AU Monitor

Plate 4 shows a 54-day comparison (October 17 to November 30, 1975) between *Dst* predicted from the Burton et al. formula (red trace) using 1-hour resolution solar wind data from Helios A and observed *Dst* (black trace). During this period, Helios A is between ~13° and ~5° east of the Earth-Sun line, is 9° to 3° north of the ecliptic, and varies in radial distance from ~0.6 to ~1.0 AU. The forecast lead time changes from ~2 days to ~1 hour during the period shown. Solar wind velocity ρ and B_z have been scaled to 1.0 AU before calculating *Dst*. Because of the long time that Helios A spends near the Earth-Sun line and the variation in radial and angular separation between Helios A and Earth, this pass provides an opportunity to evaluate the merits of various locations of an upstream solar wind monitor.

When Helios A is at radial distances between ~0.6 and ~0.7 AU (October 17-27), it is ~8° north of the ecliptic and ~10° east of the Earth-Sun line. The *Dst* predictions and observations agree in the level of activity, but the correspondence in predicted and observed variation is not clear. From 0.7 to 0.8 AU (October 28 to November 9), Helios A is ~6° north of the ecliptic and ~7° east of the Earth-Sun line. The agreement between predicted and observed *Dst*, the level of activity, and the timing of changes is not as good as we saw in section 2.2 with PVO at a similar distance. PVO was very near the ecliptic during the period discussed, whereas Helios A is ~6° north of the ecliptic. Since the average solar wind is not latitudinally uniform [*Woo, 1988*], it is possible that the solar wind conditions sampled by Helios A are not observed at Earth.

When Helios is between ~0.8 and 1.0 AU (November 10-30), it travels from ~6° north to ~3° north of the ecliptic. Helios-A is at its closest approach to the Earth-Sun line (~5°) on November 9-13. During this period, Helios predicts well the general level of activity and the timing of events, although the magnitude of one event on November 23-24 is predicted to be much stronger than it was observed to be. Note that the interplanetary shock occurring at 1340 UT on November 8, 1975 (identified by *Volkmer and Neubauer* [1985], produces a predicted 40-nT increase in *Dst*. One day later, a ~30-nT increase is observed as the interplanetary shock passes 1.0 AU. Although the forecast lead time varies from ~1 day (November 10) to ~6 hours (November 28) as the radial separation between Helios and Earth decreases, on November 17 the observations appear to precede the predictions. We attribute these differences to the rather short scale length for magnetic changes in the solar wind.

The explanation behind the observation at 1.0 AU that the stream interaction effects are seen prior to the time predicted may

be found by considering the characteristics of the stream interface that passes the Helios-A spacecraft on 18 November, 1975. If the interface is perpendicular to the ecliptic plane (upstream normal to the interface lies in the ecliptic plane), as it corotates with the Sun, it will first pass the easternmost spacecraft (Helios A in this case), then it will pass Earth. This will be the case even if the easternmost spacecraft does not lie in the ecliptic plane. However, stream interfaces are often at angles other than 90° with respect to the ecliptic [*Pizzo*, 1982]. If the interface is tilted beyond perpendicular (upstream normal points north of the ecliptic plane), it is possible that Earth will detect the interface prior to the easternmost spacecraft (assuming this spacecraft is north of the ecliptic as is Helios A). If the interface is tilted less than perpendicular (upstream normal points south of the ecliptic plane), it is possible that Earth will detect the interface after the easternmost spacecraft. To be seen simultaneously at Helios A and Earth, an interface observed on November 18 would need to be tilted such that the normal is ~51° north of the ecliptic given the position of Helios A with respect to Earth. However, comparison of predicted and observed *Dst* indicates that Helios A observes the interface ~6 hours after Earth observation. Therefore the stream interface must be tilted such that the normal is ~71° north of the ecliptic. Examination of the flow deflections observed by Helios A during this period show that the solar wind velocity has a large northward component prior to the interface, consistent with a tilt greater than perpendicular. Finally, we note that at the time of the large discrepancy on November 23 (day 327), there were significant data gaps in the Helios 1 data so that the predictions are less reliable at this time.

3. Discussion

The *Burton et al.* [1975] formula is simple in concept. This simplicity makes it very easy to use. The algorithm requires no large, long-term databases, uses very little computer space, and takes virtually no time to execute. The forecast lead time is determined mainly by the time it takes the solar wind to travel from the solar wind monitor to Earth, and its accuracy depends principally on the evolution or variation of the solar wind and IMF from the point of observations and the nose of the magnetosphere. This model could be used in conjunction with a model that forecasts the solar wind properties at 1 AU if a sufficiently accurate model existed. Despite the existence of ongoing research in this area, no such model has yet been developed.

Plates 1 through 4 demonstrate that despite the simplicity and inherent limitations in the Burton et al. formula, it is possible to make useful predictions of *Dst* using this formula and solar wind measurements made between ~0.7 and 1.0 AU. However, the accuracy of this extrapolation decreases as the distance between the solar wind monitor and Earth increases. Obviously, the best prediction capability is provided by a solar wind monitor that samples solar wind conditions representative of those later seen at 1.0 AU. In evaluating possible positions of solar wind monitors, we have assumed that the differences between predicted and observed *Dst* resulting from limitations in the Burton et al. formula are negligible compared to those resulting from variations in spatial orientation. This is reasonable given the good long-term comparison shown in Plate 1.

It is preferable to have a large forecast lead time. This can only be provided by a monitor as far inside 1.0 AU as possible. The inherent characteristics of the solar wind cause two problems in stationing a monitor far from 1.0 AU. First, inside ~0.5 AU, the solar wind exhibits many small-scale features which are not observed at 1.0 AU [*Schwenn*, 1990]. These features are purported to be swept up, "entrained," as the solar wind travels outward and are not seen by the time the solar wind reaches 1.0 AU [*Burlaga et al.*, 1985]. Also, characteristics in the solar wind that do not vary in a simple, radially dependent manner have a longer distance over which to change unpredictably. In contrast, the variations in the solar wind density and B_z between 0.7 and 1.0 AU are reasonably well predicted at 1.0 AU using the simple assumption of r^2 and r^1 variation. So, although the separation between Helios A and the ecliptic plane may have biased the conclusion that monitor positions inside ~0.7 AU are not useful, the known properties of the solar wind lead us to conclude that a solar wind monitor should be placed at least beyond 0.5 AU.

Forecast lead time is also dependent upon the type of large-scale solar wind phenomena being observed. This is because the transit time from the solar wind monitor to 1.0 AU varies according to both the speed of the solar wind and the geometry of the disturbance relative to the spacecraft and Earth. When the solar wind monitor and Earth are in near alignment, the time delay between observations of an ICME at the two locations is just that determined by the velocity of the ICME which is presumed to travel radially outward. Typically, in the data examined here, no east/west timing bias is seen with regard to ICME observations. Stream interactions are corotational solar wind features, so that the simple time delay between observations at the monitor and 1.0 AU will depend upon the radial separation as well as the east/west separation angle between the monitor and Earth. For example, when Venus is eastward to just westward of the Earth-Sun line, PVO will observe the stream interaction first. The stream interaction will then be observed at Earth at a time determined by the angular separation between Earth and Venus and the corotational speed and Archimedean spiral angle of the interaction region. As PVO travels from east to west of the Earth-Sun line, the time between observations at 0.7 AU and 1.0 AU will decrease. When PVO is ~18° west of the Earth-Sun line, the stream interaction may be detected nearly simultaneously at 0.7 AU and 1.0 AU. Thus a useful solar wind monitor should be deployed no farther west of the Earth-Sun line than ~18° at 0.7 AU. To provide the largest forecast lead time for both ICMEs and stream interaction passages, the monitor should be placed east of the Earth-Sun line but not so far east that the characteristics of the solar wind are uncorrelated with those that intersect Earth.

4. A Solar Wind Monitor

Solar wind monitor placement generates another problematic issue as a consequence of the fact that the most appropriate location for a monitor is near the ecliptic plane and near radial alignment with the Earth-Sun line during the entire year. This means that the monitor must have the same angular velocity as Earth. In a Keplerian orbit, the angular velocity of a satellite orbiting the Sun (accounting only for the gravitational effects of the Sun) is determined by the balance between the centrifugal force of the spacecraft (F_c) and the gravitational force of the Sun (F_g).

$$m\omega^2 r = GMm/r^2 \quad (1)$$

Here r is the heliocentric distance of the spacecraft, m is the mass

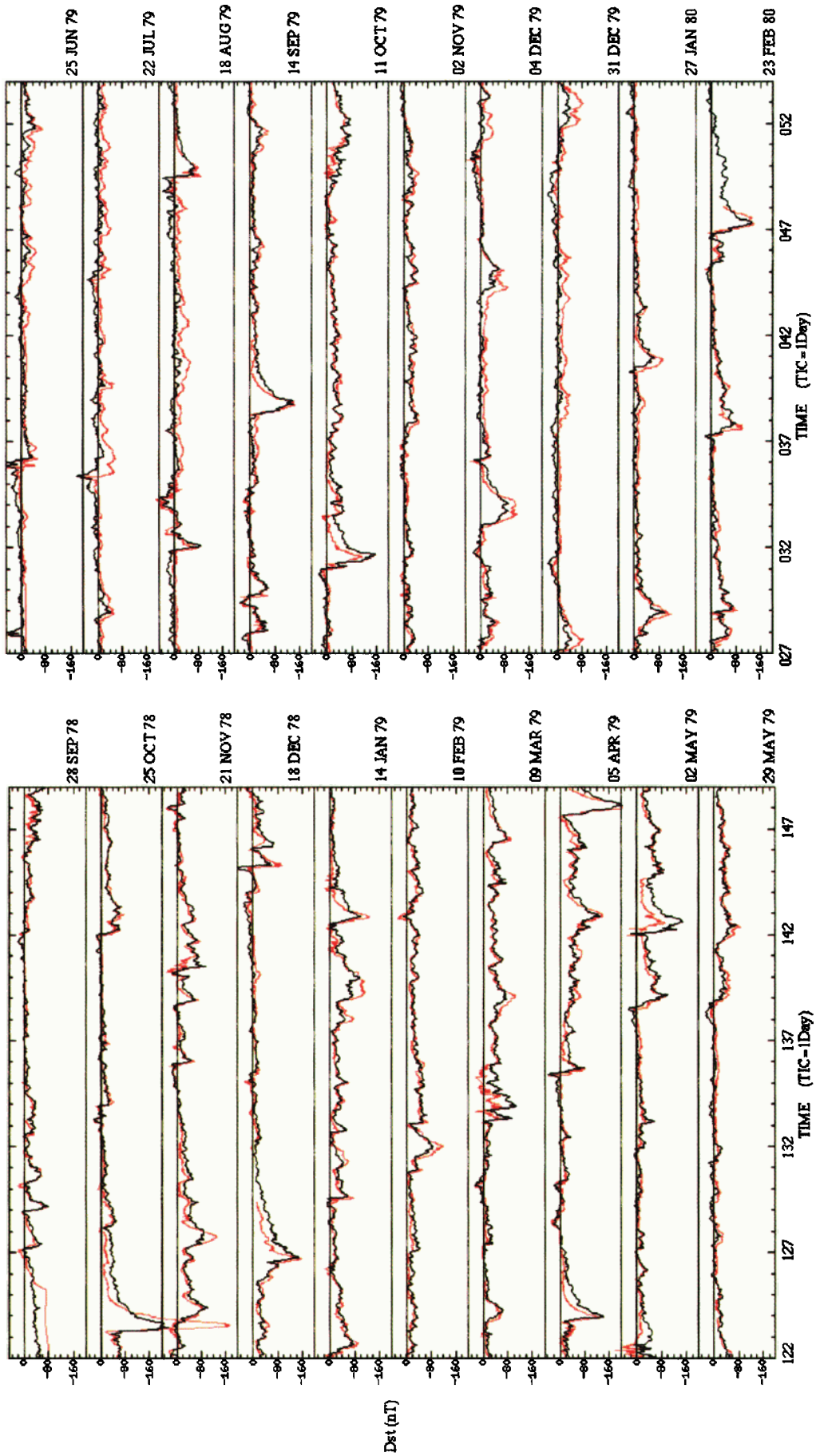

Plate 1. A 540-day comparison between observed *Dst* (black) and predicted *Dst* (red) obtained from 5-min resolution ISEE 3 solar wind measurements September 1, 1978 – February 23, 1980. Each data strip is 27 days.

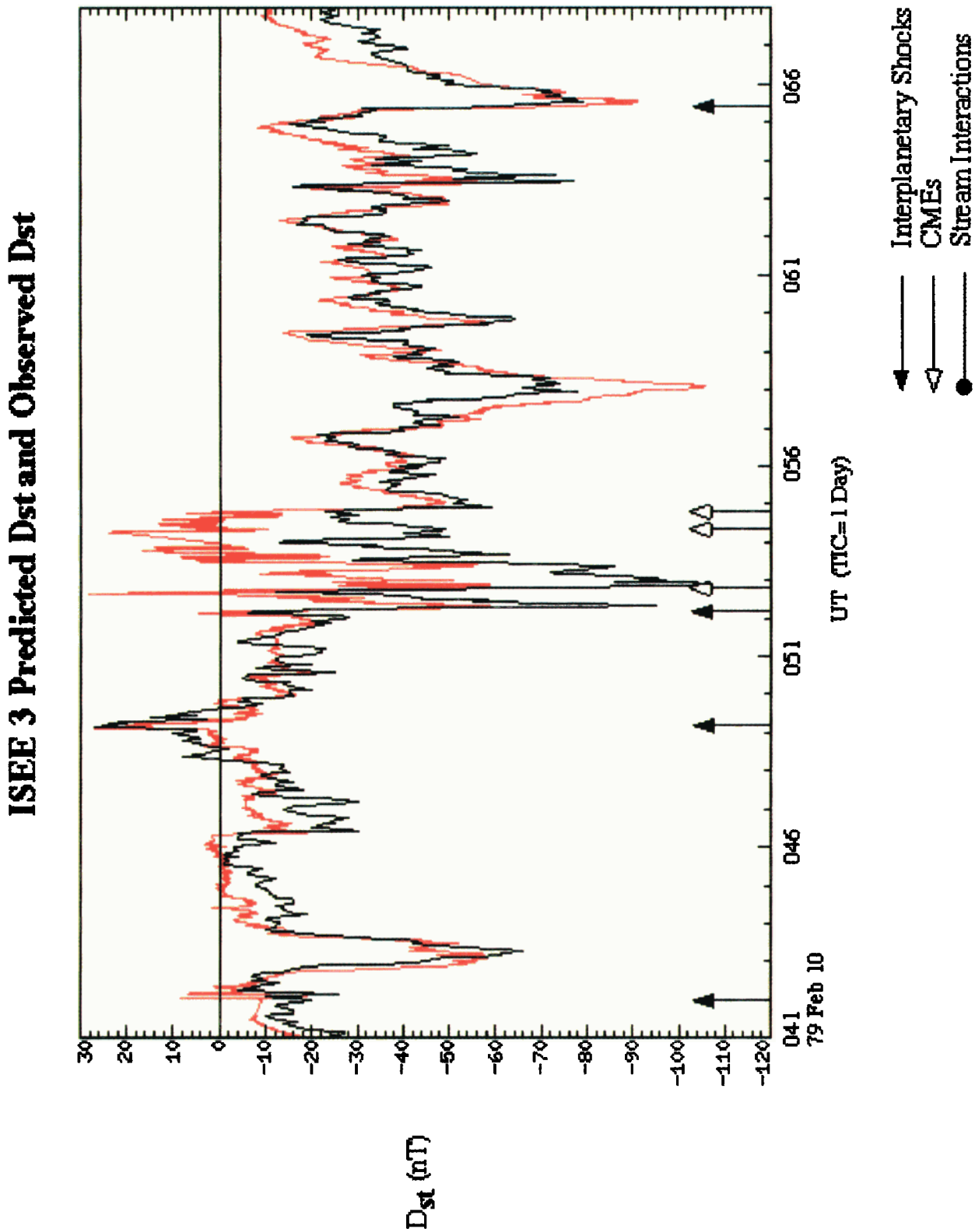

Plate 2. A 27-day interval (February 10 - March 9, 1978) extracted from the 540-day period in Plate 1.

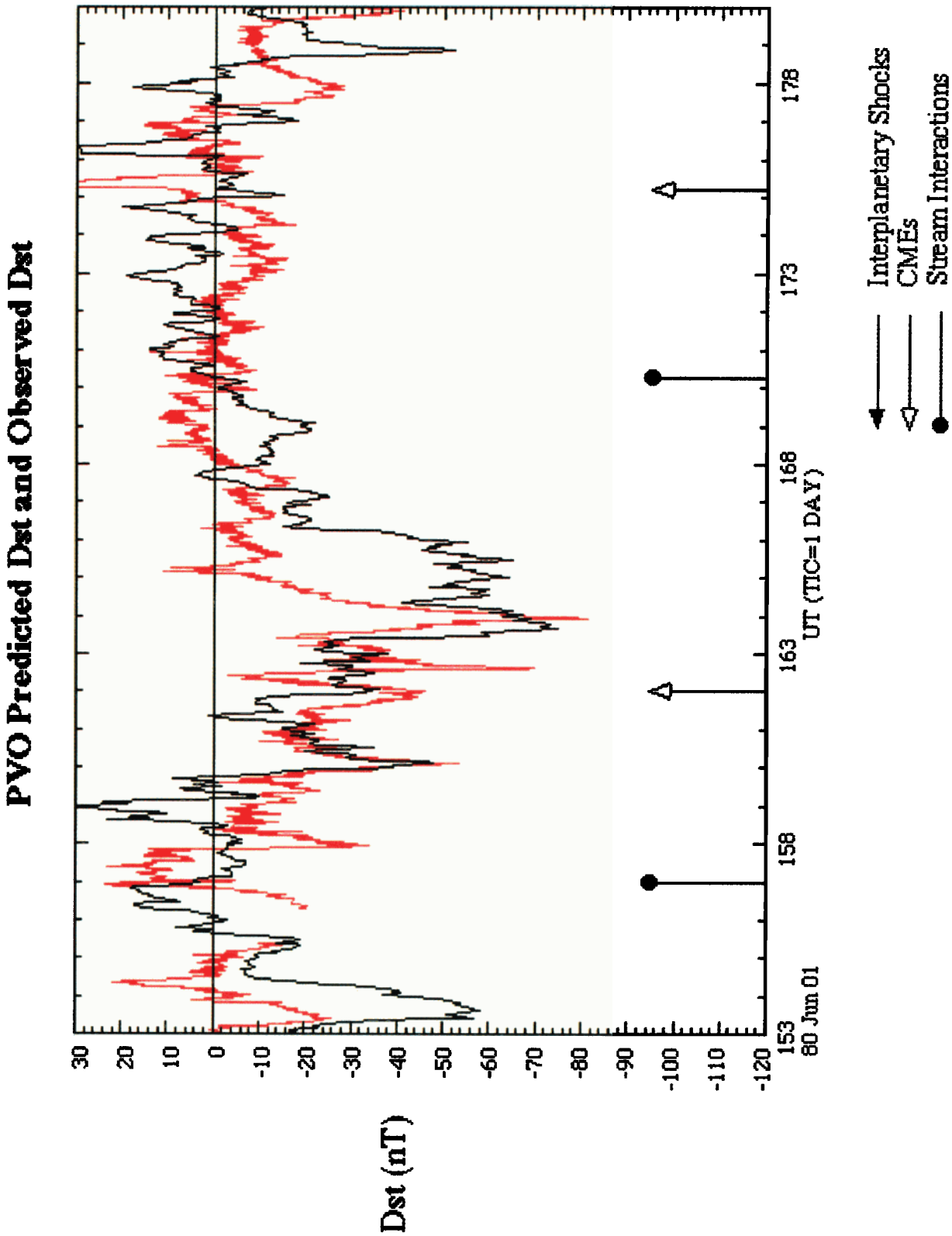

Plate 3. A 27-day comparison between observed *Dst* (black) and predicted *Dst* (red) obtained from 10-min resolution PVO solar wind measurements at 0.7 AU from June 1 - June 28, 1980.

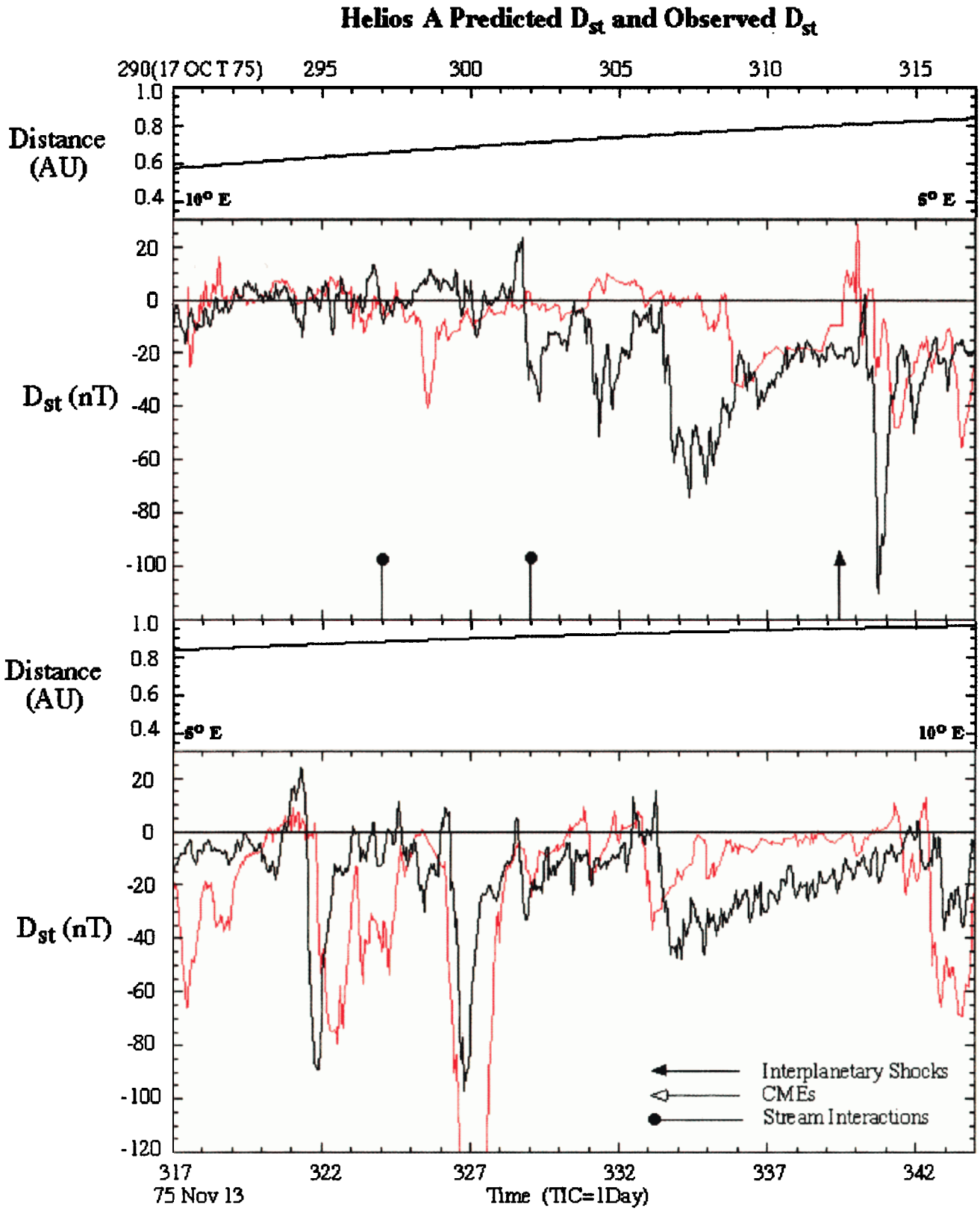

Plate 4. A 54-day comparison between observed *Dst* and predicted *Dst* using 1-hour resolution Helios A solar wind measurements from 0.6 to 1.0 AU October 17 – November 30, 1975.

of the spacecraft, M is the mass of the Sun, ω is the angular velocity of the spacecraft, and G is the universal gravitational constant. A spacecraft orbiting inside the orbit of Earth has an angular velocity greater than that of Earth. Thus, to keep a solar wind monitor synchronous with Earth about the Sun, its angular velocity about the Sun must be slowed. At the L1 libration point where SOHO and ACE are presently stationed, their angular velocity is reduced by the gravitational pull of Earth. At distances closer to the Sun than the L1 point, other means of reducing the inward pull of the Sun must be found in order to achieve Earth orbital synchronization.

Non-Keplerian orbits are possible using thrust vectoring for continuous station keeping. However, conventional technology for continuous station keeping is expensive because of the fuel required to counteract the solar-gravitational pull throughout the duration of a long mission and the additional launch costs exacted by the higher spacecraft weight. Innovative technologies such as solar wind sails could provide a practical alternative for this type of application. A solar sail provides a large area against which the Sun's radiation pressure acts. The solar photon force thus provides an outward force in addition to the centrifugal force. The orbital force balance of the spacecraft (equation (1)) then becomes

$$m\omega^2 r + P_s = GMm/r^2 \quad (2)$$

where P_s is the radiation pressure of the Sun acting on the solar sail. Expressed in terms of distance R, measured in AU, and the irradiance of the Sun at 1 AU I, (2) becomes

$$m\omega^2 R R^3_{1\,AU} + 2IA R^2_{1\,AU}/R^2 c = GMm/R^2 \quad (3)$$

where A is the area of the sail in square meters, I is 1.38×10^3 W m^{-2}, c is the speed of light and $R_{1\,AU}$ is 1.496×10^{11} m. The solar pressure force acts in conjunction with the centrifugal force to balance solar gravity and slow the spacecraft, making it possible to have a solar wind monitor inside 1 AU yet orbiting synchronously with Earth at 1.991×10^{-7} radians s^{-1}.

Solar sail technology has the advantage over conventional technology in that there are no fuel requirements for this type of station keeping. Solar sails do have mass that must be accounted for in the spacecraft mass budget. As seen from (3), the closer a spacecraft gets to the Sun (r gets smaller), the larger the sail area (A_S) must become to maintain a constant orbital speed (e.g., to keep the monitor synchronous with the orbit of Earth). For example, if a mass of 25 kg is the allowable mass of a solar sail, Joel Sercel of Jet Propulsion Laboratory, Pasadena, California, (personal communication, 1994) has estimated that a solar wind monitor could be stationed at ~0.98 AU using a solar sail of $\sim 2.3 \times 10^3$ m^2 in area. Currently produced materials are available with area densities of ~10 g m^{-2}. This produces a sail mass of ~23 kg. The present practical lower limit on surface density appears to be about 3 g m^{-2} [*Harris*, 1995]. A monitor at ~0.98 AU provides ~2.5 hours of forecast lead time on average (~1.25 hours for high-speed ICMEs). A solar wind monitor at ~0.75 AU would provide a more desirable forecast lead time of ~25 hours on average (~12 hours for high-speed ICMEs). To station a monitor at ~0.75 AU, a sail with an area of $\sim 1.8 \times 10^4$ m^2 is required. This implies a maximum allowable area density of 1.3 g m^{-2}. Sail materials of this low area density are not currently available, but are forecast to be available in the near future.

5. Conclusion

Marubashi [1989] notes that the keys to the establishment of space weather forecasting systems are (1) the development of an efficient algorithm for predictions of critical solar and geophysical phenomena and (2) secure, continuous streams of real-time data required for the prediction algorithm. In its current form, the *Burton et al.* [1975] formula provides the first key. It is simple, fast, and based solely upon solar wind measurements; it generally predicts *Dst* to within a few nanoteslas of the observed *Dst*. Thus a "magnetospheric" storm can presently be readily predicted. Deployment of an upstream solar wind monitor that would remain substantially inside 1.0 AU (0.7 to 0.95 AU), near the ecliptic plane, and orbit about the Sun synchronously with Earth providing an ongoing capability to make these predictions would be the second key toward establishing a true space weather forecast system. Such a monitor will provide useful predictions of the energization of the magnetosphere by large-scale interplanetary structures.

Acknowledgments. This work was supported by the National Aeronautics and Space Administration under grant NAGW3492-PVO and by the Los Alamos National Laboratory/Institute of Geophysics and Planetary Physics under grant 4-443869-JL-69895-03.

Hiroshi Matsumoto thanks K. Marubashi and G. Siscoe for their assistance in evaluating this paper.

References

Akasofu, S. -I., A source of the energy for geomagnetic storms and auroras, *Planet. Space Sci., 12*, 801, 1964.

Bargatze, L. F., D. N. Baker, R. L. McPherron, and E. W. Hones Jr., Magnetospheric impulse response for many levels of geomagnetic activity, *J. Geophys. Res., 90*, 6387-6394, 1985.

Bartels, J., Terrestrial-magnetic activity and its relations to solar phenomena, *J. Geophys. Res., 37*, 1-52, 1932.

Burlaga, L. F., V. J. Pizzo, A. Lazarus, and P. Gazis, Stream dynamics between 1 AU and 2 AU: A comparison of observations and theory, *J. Geophys. Res., 90*, 7377-7388, 1985.

Burton, R. K., R. L. McPherron, and C. T. Russell, An empirical relationship between interplanetary conditions and *Dst, J. Geophys. Res., 80*, 4204-4214, 1975.

Clauer, C. R., R. L. McPherron, C. Searls, and M. G. Kivelson, Solar wind control of auroral zone geomagnetic activity, *Geophys. Res. Lett., 8*, 915-918, 1981.

Crooker, N. U., G. L. Siscoe, C. T. Russell, and E. J. Smith, Factors controlling degree of correlation between ISEE 1 and ISEE 3 interplanetary magnetic field measurements, *J. Geophys. Res., 87*, 2224-2230, 1982.

Gosling, J. T., D. N. Baker, S. J. Bame, W. C. Feldman, and R. D. Zwickl, Bidirectional solar wind electron heat flux events, *J. Geophys. Res., 92*, 8519 - 8535, 1987.

Harris, H. M. (Ed.), Coronal transients and space weather prediction missions, *JPL D-12611*, Jet Propul. Lab., Pasadena, Calif., 1995.

Hirshberg, J., and D. S. Colburn, Interplanetary field and geomagnetic variations - A unified view, *Planet. Space Sci., 17*, 1183-1206, 1968.

Hoeksema, J. T., Large-scale structure of the heliospheric magnetic field: 1976-1991 in *Solar Wind VII*, edited by E. Marsch and R. Schwenn, pp. 191-196, Pergamon, Tarrytown, N.Y., 1992.

Klein, L. W., and L. F., Burlaga, Interplanetary magnetic clouds at 1 AU, *J. Geophys. Res., 87*, 613-624, 1982.

Lindsay, G. M., C. T. Russell, and J. G. Luhmann, Coronal mass ejection and stream interaction region characteristics and their potential geomagnetic effectiveness, *J. Geophys. Res., 100*, 16999-17013, 1995.

Marubashi, K., Structure of the interplanetary magnetic clouds and their solar origins, *Adv. Space Res., 68*, 335-338, 1986.

Marubashi, K., The space weather forecast program, *Space Sci. Rev., 51*, 197-214, 1989.

Paschmann, G., I. Papamastorakis, W. Baumjohann, N. Sckopke, C. W. Carlson, et al., The magnetopause for large magnetic shear: AMPTE/IRM observations, *J. Geophys. Res., 91*, 11009-11115, 1986.

Pizzo, V. J., A three-dimensional model of corotating stream in the solar wind, 3,. Magnetohydrodynamic streams, *J. Geophys. Res., 87*, 4374-4394, 1982.

Russell, C. T., R. L. McPherron, and R. K. Burton, On the cause of geomagnetic storms, *J. Geophys. Res., 79*, 1105-1109, 1974.

Russell, C. T., G. L. Siscoe, and E. J. Smith, Comparison of ISEE 1 and 3 interplanetary magnetic field observations, *Geophys. Res. Lett., 7*, 381-384, 1980.

Schwenn, R., Large-scale structure of the interplanetary medium, in *Physics of the Inner Heliosphere I*, edited by R. Schwenn, and E. Marsch, pp.99-181, Springer-Verlag, New York, 1990.

Scurry, L., and C. T. Russell, Proxy studies of energy transfer to the magnetosphere, *J. Geophys. Res., 96*, 9541-9548, 1991.

Scurry, L., C. T. Russell, and J. T. Gosling, Geomagnetic activity and the beta dependence of the daysıde reconnection rate, *J. Geophys. Res., 99*, 14811-14814, 1994.

Siscoe, G. L., A unified treatment of magnetospheric dynamics with applications to magnetic storms, *Planet. Space Sci., 14*, 947-967, 1966.

Volkmer, P. M., and F. M. Neubauer, Statistical properties of fast magnetoacoustic shock waves in the solar wind between 0.3 AU and 1 AU: Helios-1, 2 observations, *Ann. Geophys. Ser. 3, 1-12*, 1985.

Woo, R., A synoptic study of Doppler scintillation transients in the solar wind, *J. Geophys. Res., 93*, 3919-3926, 1988.

G.M. Lindsay, HQ AFSPC/DRFS, 150 Vandenberg St., Suite 1105, Peterson AFB, CO 80914-4590 (glindsay@spacecom.af.mil)

J.G. Luhmann, Space Sciences Laboratory, University of California, Grizzly Peak Blvd. at Centennial Dr., Berkeley, CA 94720 (jgluhman@ssl.berkeley.edu)

C.T. Russell, Institute of Geophysics and Planetary Physics, Uniıversity of California Los Angeles, 3845 Slichter Hall, Los Angeles, CA 90095-1567 (ctrussel@igpp.ucla.edu)

(Received October 27, 1998; revised December 25, 1998;
accepted December 28, 1998.)